J|A|C|S
ARTICLES
Published on Web 06/18/2003

Reversible Sequence of Intramolecular Associative and Dissociative Electron-Transfer Reactions in Hydrotris(Pyrazolylborate) Complexes of Rhodium

William E. Geiger,*,† Nicole Camire Ohrenberg,† Brett Yeomans,†
Neil G. Connelly,*,‡ and David J. H. Emslie‡

Contribution from the Department of Chemistry, University of Vermont, Burlington, Vermont 05405, and School of Chemistry, University of Bristol, Bristol United Kingdom BS8 1TS

Received April 4, 2003; E-mail: wgeiger@zoo.uvm.edu; neil.connelly@bristol.ac.uk

Abstract: The one-electron chemically reversible oxidation of four neutral [RhLL′(κ^2-Tp^{Me2})]complexes {Tp^{Me2} = hydrotris(3,5-dimethylpyrazolyl)borate}, which leads to κ^3-Tp^{Me2} bonding in the corresponding monocations, has been studied by cyclic voltammetry (CV) and other electrochemical methods. The CV behavior of [Rh(CO){$P(OPh)_3$}Tp^{Me2}] (**1**) and [Rh(CO)(PPh_3)Tp^{Me2}] (**2**) is quasi-nernstian at slow CV scan rates, with heterogeneous charge-transfer rates, k_s, of 0.025 cm s^{-1} and 0.015 cm s^{-1} (at 273 K), respectively. By contrast, [Rh(CO)(PCy_3)Tp^{Me2}] (**3**, Cy = cyclohexyl) and [Rh(PPh_3)$_2$$Tp^{Me2}$] (**4**) display electrochemically irreversible CV curves that arise from rate-limiting slow electron-transfer reactions. Both the oxidation of **3** (or **4**) and the rereduction of $\mathbf{3}^+$ (or $\mathbf{4}^+$) have two-step (EC-type) mechanisms in which the electron transfer (e.t.) process is followed by a separate structural change, leading to an overall square scheme with irreversible charge-transfer kinetics. Homogeneous redox catalysis was used to determine the $E_{1/2}$ value of the oxidation of **3** to an intermediate $\mathbf{3C}^+$ which is postulated to have a pseudo-square pyramidal structure. Digital simulations gave $k_s = 9 \times 10^{-3}$ cm s^{-1} for the heterogeneous charge-transfer rate of $\mathbf{3/3C}^+$. The close-to-nernstian CV behavior of **1** is ascribed to the fact that, unlike the sterically constrained derivatives **3** and **4**, the third pyrazolyl ring in **1** is already in a configuration which favors formation of the Rh−N(2) bond in $\mathbf{1}^+$. The overall redox mechanism for this series of compounds involves an associative oxidative e.t. reaction followed by a dissociative reductive e.t. process.

Introduction

An electron transfer (e.t.) reaction which displays irreversible voltammetry does so because of slow heterogeneous electron-transfer kinetics and/or a fast chemical reaction following the charge-transfer step.[1] A dissociative e.t. process (i.e., one involving *bond cleavage*) is a subset of irreversible processes important both for conceptual reasons and for the relevance of bond-altering e.t. processes in numerous chemical and biological reactions.[2] Even a cursory examination of the literature reveals the complexities involved in addressing the mechanisms of dissociative e.t. processes.[2c,2d,2e,3] If X−Y bond cleavage is concomitant with electron transfer, the "concerted" single-step (E) reaction of eq 1 applies and the standard heterogeneous e.t. rate constant, k_s, may be used within the Marcus theory[4] to estimate the energy of the fractured bond.[5] Because the alternate "consecutive" or "two-step" (EC) mechanism of eq 2 cannot directly yield such information, there is ongoing interest in determining the mechanisms of irreversible e.t. processes.[2d,2e,5] The most detailed

$$X{-}Y + e^- \rightarrow X + Y^- \text{ "concerted", E} \quad (1)$$

$$X{-}Y + e^- \rightleftharpoons [X{-}Y]^- \rightarrow X + Y^- \text{ "consecutive", EC} \quad (2)$$

studies to date involve reactions linked to an essentially irreversible bond cleavage, e.g., the one-electron reductive fragmentation of halocarbons[2c,2d,2e,5,6] or sulfonium ions.[5,6] It

† University of Vermont.
‡ University of Bristol.

(1) Bard, A. J.; Faulkner, L. R. *Electrochemical Methods*; John Wiley and Sons: New York, 2001, 2nd edition, p 161.
(2) Leading references: (a) Armstrong, F. A. *J. Chem. Soc., Dalton Trans.*, **2002**, 661 (b) Davidson, V. L. *Acc. Chem. Res.* **2000**, *33*, 87 (c) Savéant, J.-M. *Advances in Electron-Transfer Chemistry*; Mariano, P. S., Ed.; JAI Press: New York, 1994; Vol. 4, p 53 (d) Savéant, J.-M. *Adv. Phys. Org. Chem.* **2000**, *35*, 117 (e) Eberson, L. *Acta Chem. Scand.* **1999**, *53*, 751 (f) Gaillard, E. R.; Whitten, D. G. *Acc. Chem. Res.* **1996**, *29*, 292 (g) Williams, A. *Chem. Soc. Rev.* **1994**, *23*, 93 (h) Karki, S. B.; Dinnocenzo, J. P.; Farid, S.; Goodman, J. L.; Gould, I. R.; Zona, T. A. *J. Am. Chem. Soc.* **1997**, *119*, 431 (i) Costentin, C.; Hapiot, P.; Mèdebielle, M.; Savéant, J.-M. *J. Am. Chem. Soc.* **1999**, *121*, 4451 (j) Hoffman, B. M.; Ratner, M. A. *J. Am. Chem. Soc.* **198**7, *109*, 6237 (k) Hoffman, B. M.; Ratner, M. A.; Wallin, S. A. *Adv. Chem. Ser.* **1990**, *226*, 125 (l) Razavet, M.; Borg, S. J.; George, S. J.; Best, S. P.; Fairhurst, S. A.; Pickett, C. J. *Chem. Commun.* **2002**, 700.
(3) Wang, X.; Saeva, F. D.; Kampmeier, J. A. *J. Am. Chem. Soc.* **1999**, *121*, 4364.
(4) (a) Marcus, R. A. *Annu. Rev. Phys. Chem.* **1964**, *15*, 155 (b) ref 1, pp 117−124 (c) Hale, J. M. In *Reactions of Molecules at Electrodes*; Hush, N. S., Ed.; Wiley-Interscience: London, 1971; pp 229-ff. For the standard heterogeneous e.t. rate we use the term k_s, although k° is often employed in the literature.[1.]
(5) Savéant, J.-M *Acc. Chem. Res.* **1993**, *26*, 455.
(6) (a) Maran, F.; Wayner, D. D. M.; Workentin, M. S. *Adv. Phys. Org. Chem.* **2001**, *36*, 85 (b) Robert, M.; Savéant, J.-M. *J. Am. Chem. Soc.* **2000**, *122*, 514 (c) Daley, C. J. A.; Holm, R. H. *Inorg. Chem.* **2001**, *40*, 2785.

 10.1021/ja0302073 CCC: $25.00

Scheme 1

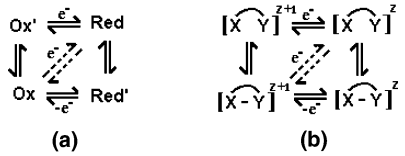

is desirable to extend these inquiries to *chemically reversible* e.t. processes involving molecules with single breakable (frangible[7]) bonds.

The general case of electron transfer coupled to a reversible structural change can usually be treated as the four-membered square scheme of Scheme 1(a). In this scheme, the concerted single-step (E) mechanism uses only the diagonal redox direction between Red and Ox, whereas the consecutive two-step model involves four structures (Red, Ox′, Ox and Red′) in a pair of EC mechanisms ($E_{ox}C/E_{red}C$). Scheme 1b adapts this model to the present discussion of a reversible bond-fracture process. In this representation, the X−Y bond is fully formed in the oxidation leading to the $(z + 1)$ charge state and fully cleaved in the reduction leading to the z charge state. The elongation of the bond does not result in loss of either atom from the redox species.

The rich literature of electron-transfer square schemes[7,8] includes little on systems in which the structural effects might be considered to be similar to a "simple" bond alteration such as C-halogen cleavage.[5,9] One loose analogy is that of the e.t.-induced hapticity changes (e.g., η^6/η^4 or η^5/η^3 ring slippage) in metal-π-polyolefin compounds.[10−12] Metal π-systems, however, usually exhibit rather fast one-step redox reactions owing to the presence of relatively accessible e.t. transition states. For example, the impressive energetic ease of π-hapticity changes has recently been noted for η^n- indenylmolybdenum compounds which traverse the η^3 to η^4 to η^5 bonding modes as the metal center undergoes successive one-electron oxidations.[12]

Energetically more demanding, but still chemically reversible, making and breaking of a metal−ligand bond is required to obtain models for the reversible processes of Scheme 1b. Promising candidates are the hydrotris(pyrazolyl)borate complexes of rhodium, in which a Rh(I)/Rh(II) redox couple is linked to formation and disruption of a Rh−N σ-bond. The Rh(II) compounds display κ^3-bonding of Rh to one N from each pyrazolyl ring, giving five-coordinate 17 e^- cations such as $[Rh(CO)(PPh_3)Tp^{Me2}]^+$, $\mathbf{2}^+$, Tp^{Me2} = hydrotris(3,5-dimethylpyrazolyl)borate (see 5-coordinate structure below).[13,14] The

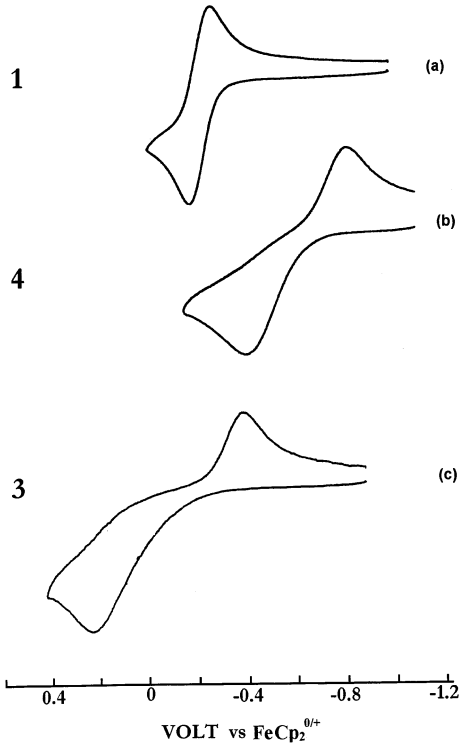

Figure 1. Qualitative comparison of cyclic voltammetry scans of (a) $[Rh(CO)\{P(OPh)_3\}Tp^{Me2}]$ (**1**), (b) $[Rh(PPh_3)_2Tp^{Me2}]$ (**4**), and (c) $[Rh(CO)(PCy_3)Tp^{Me2}]$ (**3**) in CH_2Cl_2/0.1 M $NBu_4][PF_6]$ at glassy carbon electrode, scan rate 0.2 V s^{-1}.

neutral Rh(I) compounds $[RhLL'Tp^{Me2}]$, where L or L′ is CO, a P-atom donor, or another ligand,[14,15] exhibit either strictly κ^2-bonding to the Tp^{Me2} ligand, resulting in a 4-coordinate metal, or in an equilibrium between κ^2- and weak κ^3-Tp^{Me2} coordination.[14] Changes in the ligands (either L or the substituents on the Tp ring) affect the favored structures, with more bulky ligands favoring κ^2-coordination.[14−16]

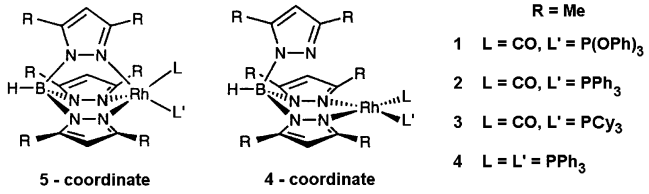

Idealized Structures and Definitions of 1-4

Idealized Structures and Definitions of 1−4. Cyclic voltammetry (CV) experiments reveal contrasting voltammetric behavior for different members of this series, ranging from *qualitatively* reversible to irreversible CVs (Figure 1), even though the various derivatives undergo the same *chemically reversible* one-electron Rh(I)/Rh(II) redox reaction of eq 3

(7) There are opposing views on whether the reverse reaction of eq 2 can be considered to be practical under the normal experimental conditions. See refs 2d and 2e for discussion. For theoretical treatment see Saveant, J.-M. *J. Electroanal. Chem.* **2000**, *485*, 86.

(8) For an excellent general review of the square scheme mechanism and the idea of the cross redox reaction, see: (a) Evans, D. H.; O'Connell, K. M. In *Electroanalytical Chemistry*; Bard, A. J., Ed.; Marcel Dekker: New York, 1986; Vol 14, pp 113 ff. See also: (b) Rieger, P. H. *Electrochemistry*; Chapman & Hall: New York, 1994; 2nd ed., p 264 and Astruc, D. *Electron Transfer and Radical Processes in Transition Metal Chemistry*; VCH Publishers: New York, 1995; pp 126−136.

(9) (a) Pause, L.; Robert, M.; Savéant, J.-M. *J. Am. Chem. Soc.* **1999**, *121*, 7158 (b) Adcock, W.; Andrieux, C. P.; Clark, C. I.; Neudeck, A.; Savéant, J.-M.; Tardy, C. *J. Am. Chem. Soc.* **1995**, *117*, 8285, and references therein.

(10) (a) Geiger, W. E. *Progress in Inorganic Chemistry*; Lippard, S. J., Ed.; John Wiley and Sons: New York, 1985; Vol. 33, p 275. (b) Geiger, W. E. *Acc. Chem. Res.* **1995**, *28*, 351.

(11) Nielson, R. M.; Weaver, M. J. *Organometallics* **1989**, *8*, 1636.

(12) Stoll, M. E.; Belanzoni, P.; Calhorda, M. J.; Drew, M. G. B.; Felix, V.; Geiger, W. E.; Gamelas, C. A.; Gonçalves, I. S.; Romão, C. C.; Veiros, L. F. *J. Am. Chem. Soc.* **2001**, *123*, 10 595, and references therein.

(13) Connelly, N. G.; Emslie, D. J. H.; Metz, B.; Orpen, A. G.; Quayle, M. J. *Chem. Commun.* **1996**, 2289.

(14) Connelly, N. G.; Emslie, D. J. H.; Geiger, W. E.; Hayward, O. D.; Linehan, E. B.; Orpen, A. G.; Quayle, M. J.; Rieger, P. H. *J. Chem. Soc., Dalton Trans.* **2001**, 670.

(15) (a) Chauby, V.; Le Berre, C. S.; Kalck, P.; Daran, J.-C.; Commenges, G. *Inorg. Chem.* **1996**, *35*, 6354. (b) Malbosc, F.; Kalck, P.; Daran, J.-C., Etienne, M. *J. Chem. Soc., Dalton Trans.* **1999**, 271.

(16) (a) Trofimenko, S. *Chem. Rev.* **1993**, *93*, 943. (b) Kitajima, N.; Tolman, W. B. *Progress in Inorganic Chemistry*; Karlin, K., Ed.; John Wiley and Sons: New York, 1995; Vol. 43, p 419.

$$[RhLL'(\kappa^2\text{-}Tp^{Me2})] \rightleftharpoons [RhLL'(\kappa^3\text{-}Tp^{Me2})]^+ + e^- \quad (3)$$

We have examined four members of this series, including the monosubstituted triphenyl phosphite (**1**) and triphenylphosphine (**2**) complexes which exhibit *quasi-nernstian* CV behavior.[17] The tricyclohexylphosphine complex, **3**, and the bis(triphenylphosphine) complex, **4**, both have very large CV peak separations and follow *totally irreversible*[17] electron-transfer kinetics. In this work, it is shown that $z = 0/+$ charge-transfer in [Rh(CO)(PCy$_3$)Tp^{Me2}] (**3**) or [Rh(PPh$_3$)$_2$Tp^{Me2}] (**4**) must follow two-step mechanisms in an overall square scheme. No firm mechanistic conclusions can be made about the more rapid electron-transfer processes of [Rh(CO)P(OPh)$_3$Tp^{Me2}] (**1**) and [Rh(CO)(PPh$_3$)Tp^{Me2}] (**2**), for which either one-step or two-step models are consistent with experimental findings. Ligand steric properties are invoked to account for the apparent differences in voltammetric behavior.

Experimental Section

Compounds **1**−**4** were prepared as described earlier.[14] All voltammetric measurements were carried out under nitrogen, using either Schlenk or drybox conditions. THF was distilled from purple solutions of Na/benzophenone and dichloromethane was distilled from CaH_2. The supporting electrolyte was 0.1 M [NBu$_4$][PF$_6$]. In this paper all potentials are referenced to that of the ferrocene/ferrocenium couple.[18] The experimental reference electrode was either the S.C.E. or a Ag/AgCl electrode fabricated by electrodepositing AgCl on a silver wire. In many cases the [FeCp$_2$] $^{0/+}$ potential was obtained by adding ferrocene to the test solution at an appropriate time in the experiment. The S.C.E. was used under Schlenk conditions at room temperature for experiments in which addition of ferrocene to the solution produced or was likely to produce a change in the behavior of the analyte (vide infra). In those cases (all involving CH_2Cl_2 as solvent), 0.46 V was subtracted from the measured potential to convert it to the $[FeCp_2]^{0/+}$ reference. In some cases, decamethylferrocene was the experimental reference of choice. In CH_2Cl_2/0.1 M [NBu$_4$][PF$_6$], we measure the $E_{1/2}$ of $[Fe(\eta^5\text{-}C_5Me_5)_2]^{0/+}$ as −0.55 V vs ferrocene. Because some electrode history was noted for the Rh analytes at Pt or Au electrodes, a glassy carbon disk of $d = 1-2$ mm, polished when needed, was used for all the data reported in this paper. Rate constants for the homogeneous redox catalysis (HRC) interaction of **3** with a mediator (either $[Pd\{S_2C_2(CN)_2\}_2]^{2-}$, ferrocene, or ferrocenylacetonitrile, [Fe(η^5-C$_5$H$_4$CH$_2$CN)(η^5-C$_5$H$_5$)]), were obtained by measuring anodic CV peak heights or limiting steady-state currents for mixtures of **3** and the mediators. A scan rate of 1 mV s^{-1} was used for the steady-state scans. Concentrations of 0.3 mM for **3** and 0.1 mM to 1.0 mM for $[Pd\{S_2C_2(CN)_2\}_2]^{2-}$ gave changes in steady-state currents (or CV currents using scan rates of 0.1 to 3 V s^{-1}) in a suitable range so that the working curves of Savéant and co-workers[19] could be employed to measure the value of k_f (eq 5). Concentrations in the HRC experiments were (a) 0.16 mM to 1.3 mM for **3** and 0.65 mM for ferrocene, (b) 0.3 mM for **3**, 0.1 mM to 0.75 mM ferrocenylacetonitrile. The k_f value for **3** and ferrocene was confirmed by digital simulations using Digisim version 3.1 (Bioanalytical Systems). Details of general electrochemical methodologies are available elsewhere.[20, 21]

Scheme 2

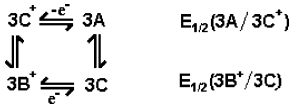

Results and Discussion

Overview of Results. The known structural preferences of this class of compounds aid in understanding the redox mechanisms. Three limiting structures are considered to be the most stable for the Rh(I) and Rh(II) complexes. Whereas the κ^2 square planar structure **A** is preferred[22(a)] for the neutral complexes **2**, **3**, and **4**, the idealized square-pyramidal κ^3-structure **B** is found for all four Rh(II) cations.[14] Compound **1**, [Rh(CO)P(OPh)$_3$Tp^{Me2}], has the distorted square-pyramidal structure **C**, roughly between structures **A** and **B**, in which the Rh-to-apical-nitrogen distance of 2.764 Å signifies a weak bond.[22] The intermediate necessary to account for the redox reactions of **3** and **4** is likely to have a pseudo-square-pyramidal geometry similar to that of **C**.

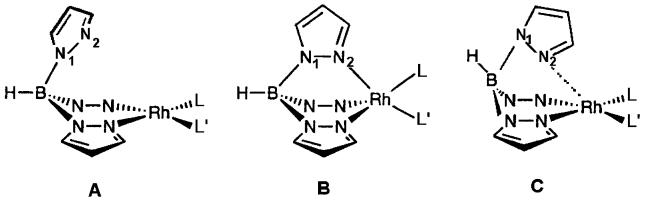

The chemical reversibility of the one-electron oxidation of **1**−**4** was confirmed by cyclic voltammetry, double potential-step chronoamperometry, and bulk coulometry.[23] As shown below, the P(OPh)$_3$ and PPh$_3$ derivatives, **1** and **2**, exhibit quasi-nernstian electron-transfer behavior.[17] CV wave shapes of **1** and **2** take on a nearly ideal reversible appearance at relatively slow scan rates. In contrast, the PCy$_3$ complex, **3**, and the bis(triphenylphosphine) complex, **4**, have anodic and cathodic features characteristic of totally irreversible[17] e.t. behavior followed by chemical reactions that are fast on the CV time scale. Accordingly, the CV results for **3** and **4** arise from an initial two-step (E_{ox}C) anodic process to give the Rh(II) monocation, followed by a subsequent two-step (E_{red}C) cathodic process back to the Rh(I) neutral compound. In Scheme 2, the structures (labeled **A**−**C** as described above) assigned to the redox process of [Rh(CO)(PCy$_3$)Tp^{Me2}] (**3**) are shown. Table 1 summarizes the potentials determined and the mechanisms assigned to **1**−**4**.

Discussion begins with [Rh(CO)(PCy$_3$)Tp^{Me2}], which has the largest separations of E_{pa} and E_{pc} in this series and was the most intensively studied.

(17) The term quasi-nernstian is used to describe a heterogeneous e.t. process that is near equilibrium, often referred to as quasireversible. In practice, a system with a relatively fast but measurable k_s value fits this description. An irreversible e.t. process is one in which the heterogeneous e.t. is the rate-determining step. In terms of CV measurements, irreversible behavior is typically followed when the ΔE_p values are greater than about 200 mV for a one-electron process at 298 K. See (a) ref 1, pp 111 ff (b) Nicholson, R. S. *Anal. Chem.* **1965**, *37*, 1351.

(18) (a) Gritzner, G.; Kuta, J. *Pure Appl. Chem.* **1984**, *56*, 461 (b) Connelly, N. G.; Geiger, W. E. *Chem. Rev.* **1996**, *96*, 877.

(19) (a) Andrieux, C. P.; Hapiot, P.; Savéant, J.-M. *Chem. Rev.* **1990**, *90*, 723. (b) Andrieux, C. P.; Dumas-Bouchiat, J. M.; Savéant, J.-M *J. Electroanal. Chem.* **1980**, *113*, 1. (c) Andrieux, C. P.; Blocman, C.; Dumas-Bouchiat, J. M.; M'Halla, F.; Savéant, J.-M *J. Electroanal. Chem.* **1980**, *113*. (d) Evans, D. H.; Gilicinski, A. G.; Evans, D. H. *J. Electroanal. Chem.* **1989**, *267*, 93. (e) Gilicinski, A. G.; Evans, D. H. *J. Phys. Chem.* **1992**, *96*, 2528.

(20) Stoll, M. E.; Lovelace, S. R.; Geiger, W. E.; Schimanke, H.; Hyla-Kryspin, I.; Gleiter, R. *J. Am. Chem. Soc.* **1999**, *121*, 9343.

(21) Geiger, W. E. In *Laboratory Techniques in Electrochemistry*; Kissinger, P. T., Heineman, W. R., Eds.; Marcel Dekker: New York, 1996 2nd ed., pp 683 ff.

(22) (a) A different type of κ^2 structure may be found in Tp-type complexes lacking Me groups in the 5-position. See ref 14 and literature therein; (b) the Rh to apical N distance in **1** (2.764 Å)[9] is within the sum (2.89 Å) of the van der Waals radius of nitrogen and the atomic radius of rhodium.

(23) Reference 14 and Geiger, W. E., unpublished work. Some decomposition of **3**$^+$ is observed under bulk electrolysis conditions at room temperature.

Table 1. Voltammetry Results for Hydrotris(pyrazolyl)boratorhodium Complexes in CH_2Cl_2/0.1 M $[NBu_4][PF_6]$ (Potentials in Volt vs$[FeCp_2]^{0/+}$)[a]

compound or product	redox mech[b]	$E_{1/2}$	E_{pa} or E_{pc}
$[Rh(CO)P(OPh)_3Tp^{Me2}]$ (**1**)	$0/+$ E_{QN}	-0.17[c]	
$[Rh(CO)(PPh_3)Tp^{Me2}]$ (**2**)	$0/+$ E_{QN}	-0.25[c]	
$[Rh(CO)(PCy_3)Tp^{Me2}]$ (**3**)	$0/+$ E_{irrev}C	0.20[d]	0.30[e]
$[Rh(PPh_3)_2Tp^{Me2}]$ (**4**)	$0/+$ E_{irrev}C	ca. -0.61 (see text)	-0.47[f]
$[Rh(CO)(PCy_3)Tp^{Me2}]^+$ ($\mathbf{3}^+$)	$+/0$ E_{irrev}C	-0.11 to -0.32 (see text)	-0.45[e]

[a] The neutral compounds were the starting analytes, whereas the cationic compounds were generated in the CV scans. E_{QN} refers to a quasi-nernstian e.t. process, E_{irrev} to an electrochemically irreversible e.t. process, and C to a chemical or structural process which is separate from the E step. [b] Charges of the *forward* electron-transfer reaction are shown; i.e., $+/0$ refers to the reduction of $\mathbf{3}^+$ to **3**. [c] Average of E_{pa} and E_{pc} at slow CV scan rates. [d] Measured by homogeneous redox catalysis method (see text). [e] E_{pa} at $\nu = 2$ V s^{-1}. [f] E_{pa} at $\nu = 0.03$ V s^{-1}.

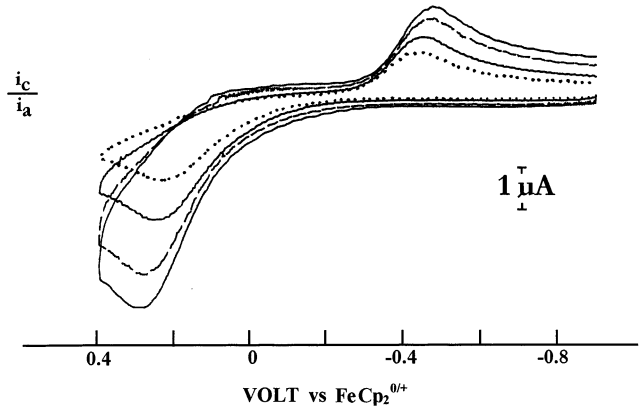

Figure 2. CV scans of 0.8 mM $[Rh(CO)(PCy_3)Tp^{Me2}]$ (**3**) in CH_2Cl_2/0.1 M $[NBu_4][PF_6]$ at glassy carbon electrode with increasing scan rates (0.4, 0.8, 1.5, and 2.0 V s^{-1})

$[Rh(CO)(PCy_3)Tp^{Me2}]$ (3). As shown in Figures 1c and 2, the CV of the PCy_3 complex **3** has a broad anodic wave and a coupled cathodic wave, the two features being separated by a large potential difference which increases with CV scan rate ($E_{pa} - E_{pc} = 600$ mV at $\nu = 0.1$ V s^{-1}; 750 mV at $\nu = 2$ V s^{-1}). Both the oxidation and reduction e.t. processes are irreversible,as determined by the shifts of E_{pa} and E_{pc} with scan rate according to eqs 4a and 4b, where ν is the CV scan rate and β and α are the charge-transfer symmetry coefficients

$$\text{oxdn: } \delta(E_{pa}/\log \nu) = (30/\beta)\ \text{mV} \qquad (4)$$

$$\text{redn: } \delta(E_{pc}/\log \nu) = (30/\alpha)\ \text{mV} \qquad (5)$$

for the anodic and cathodic reactions, respectively.[24] Slopes of 90 mV and 64 mV, respectively, for the oxidation and reduction waves gave $\beta = 0.33$ for $\mathbf{3A/3C}^+$ and $\alpha = 0.47$ for $\mathbf{3B}^+/\mathbf{3C}$.[25a] The breadths of the waves were consistent with these transfer coefficients.[25b] The consequence of these measurements is that the coupled anodic and cathodic processes *cannot* be attributed to a slow, single-step electron-transfer process, which requires that α and β sum to unity.[26] Two-step models are therefore required for both the E_{ox}C oxidation of $[Rh(CO)(PCy_3)Tp^{Me2}]$ (**3A**) and the E_{red}C reduction of $[Rh(CO)(PCy_3)Tp^{Me2}]^+$ ($\mathbf{3B}^+$)[27] under conditions of rate-determining (i.e., irreversible) electron-transfer steps. Both coupled chemical steps lie strongly in favor of the respective products and are fast on the CV time scale. The impediments to obtaining $E_{1/2}$ and k_s values for irreversible charge-transfer systems are well-known.[28] To quantitatively test the proposed $E_{ox}C/E_{red}C$ mechanism,[29] homogeneous redox catalysis (HRC) was used to determine the $E_{1/2}$ value of the $\mathbf{3A/3C}^+$ couple. The HRC method[19] takes advantage of changes in current induced by a second-order redox reaction between the analyte (in this case **3**) and added mediators (having highly reversible e.t. couples) to obtain an estimate of the $E_{1/2}$ value of the analyte. The prerequisite[19(a)] that the analyte has an electrochemically or chemically irreversible redox reaction is fulfilled by the anodic behavior of $[Rh(CO)(PCy_3)Tp^{Me2}]$.

Homogeneous Redox Catalysis (HRC): Determination of $E_{1/2}$ ($\mathbf{3A/3C}^+$). A mediator designated by the oxidized form P and the reduced form Q, added to a solution of $[Rh(CO)(PCy_3)Tp^{Me2}]$, induces the homogeneous electron-transfer reaction of eq 5

$$\mathbf{3A} + \mathrm{P} \underset{k_b}{\overset{k_f}{\rightleftharpoons}} \mathbf{3C}^+ + Q \qquad K_{HRC} = [\mathbf{3C}^+][Q]/[\mathbf{3A}][P] \quad (5)$$

If $E_{1/2}$ (Q/P) is sufficiently close to the $E_{1/2}$ of $\mathbf{3A/3C}^+$, then (i) the anodic peak current, i_{pa}, for $[Rh(CO)(PCy_3)Tp^{Me2}]$ diminishes and may be completely absent, (ii) the anodic peak current for oxidation of Q increases over its normal diffusion-controlled value, and (iii) the apparent chemical reversibility of the mediator (Q/P) couple decreases, as shown by diminution of the cathodic return peak of the mediator. All three effects were observed when any one of three different mediators in its reduced state was added to solutions of $[Rh(CO)(PCy_3)Tp^{Me2}]$.

Savéant and co-workers have provided working curves which allow determination of the analyte $E_{1/2}$ based on experimental conditions (e.g., concentrations of analyte and mediator, $E_{1/2}$ of the latter) and the measured parameter (e.g., CV or steady-state currents).[19(b),19(c)] . This approach was used for $[Rh(CO)(PCy_3)Tp^{Me2}]$ in the presence of $[Pd\{S_2C_2(CN)_2\}_2]^{2-}$ ($E_{1/2} = -0.09$ vs ferrocene),[30] ferrocene, ($E_{1/2} = 0$) or ferrocenylacetonitrile ($E_{1/2} = 0.07$ V vs ferrocene) to measure the k_f of eq 5. Alternatively, digital simulations of combined analyte/mediator solutions at different concentrations and CV scan rates were employed (see the Experimental Section for more details). Figure 3 shows the changes in the CV of ferrocene when $[Rh(CO)(PCy_3)Tp^{Me2}]$ is added, and Figure 4 reproduces the experimental and simulated fits of the anodic currents at representative scan rates for a 4.3:1 ratio of $[Rh(CO)(PCy_3)Tp^{Me2}]/[FeCp_2]$. Table 2 gives the values of k_f for the three different mediators. A plot of log k_f vs $E_{1/2}$ (Q/P) was linear with the expected slope of 60 mV, giving an $E_{1/2}$ value of 0.20 V for the $\mathbf{3A/3C}^+$ couple from the intercept at a k_f value of

(24) The β parameter is often denoted as 1-α in the literature.
(25) (a) Replicate experiments: 90 mV and 90 mV for $\mathbf{3}^{0/+}$; 62 mV and 66 mV for $\mathbf{3}^{+/0}$ over $\nu = 0.1$ V s^{-1} to $\nu = 4$ V s^{-1} (b) $\beta = 0.32$, $\alpha = 0.50$ using $|E_p - E_{p/2}| = 47/\beta$ (or α) in mV.
(26) For a discussion of transfer coefficients see ref 1, pp 97−98 and ref 8(b), pp 317−323.
(27) Although the formal diagnostics for the reverse (cathodic) process require only an E_{irrev} process, chemical intuition and the principle of microscopic reversibility require a coupled chemical reaction in the regeneration of **3**.
(28) (a) Ref 1, pp 195−197 (b) Oldham, K. B.; Myland, J. C. *Fundamentals of Electrochemical Science*, Academic Press: San Diego, 1994; pp 292−294.
(29) This designation is intended to bring attention to the two directions of the overall anodic/cathodic process.
(30) $E_{1/2} = -0.09$ V vs $FeCp_2^{0/+}$ under these conditions (see Geiger, W. E.; Barrière, F.; LeSuer, R. J.; Trupia, S. *Inorg. Chem.* **2001**, *40*, 2472). $E_{1/2} = 0.46$ V vs SCE in CH_3CN (Davison, A.; Edelstein, N.; Holm, R. H.; Maki, A. H. *Inorg. Chem.* **1963**, *2*, 1227.

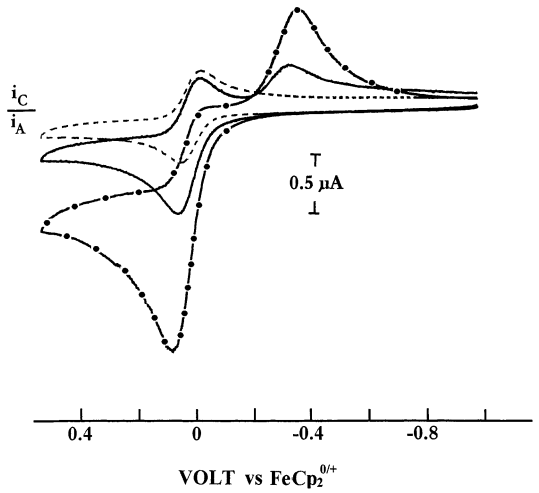

Figure 3. CV scans of 0.5 mM ferrocene in CH_2Cl_2/0.1 M $[NBu_4][PF_6]$ at glassy carbon electrode (- - -) and after addition of 2.0 equiv **3** (—) or 7.3 equiv of **3** (•—•—•—•—•), scan rate 0.2 V s^{-1}

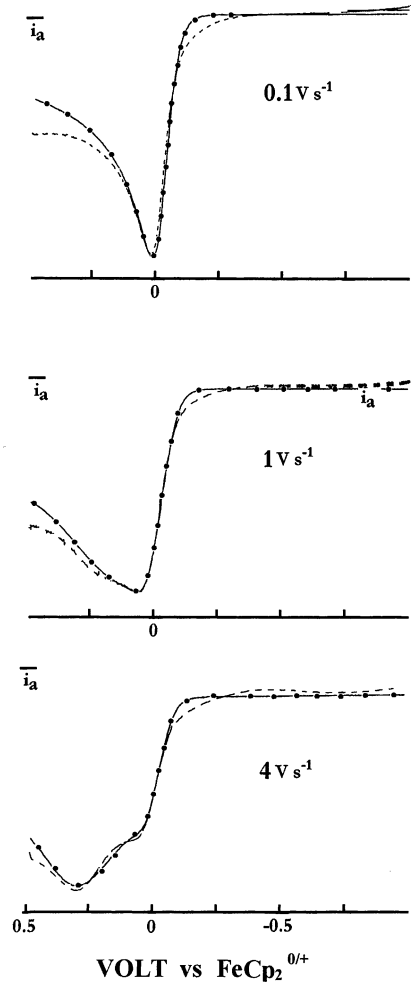

Figure 4. Anodic linear scan currents for 4.3:1 ratio of **3** to ferrocene at different scan rates. Dashed lines are experimental; —•—•—•—• is simulated with k_f (eq 6) = 3×10^5 M^{-1} s^{-1}; $E_{1/2}$ (**3A**/**3C**$^+$) = 0.21 V; k_s = 0.008 cm s^{-1}; α = 0.32 R_u= 10^4 Ω; capacitance = 0.1 μF

10^9 $M^{-1}s^{-1}$. This value of $E_{1/2}$ (**3A**/**3C**$^+$) was then used in simulations of the CV features of **3** in the *absence* of mediators to obtain a k_s value for the anodic reaction.

Digital Simulations: Determination of k_s for 3A/3C$^+$. Having in hand both the $E_{1/2}$ value (0.20 V) and the transfer coefficient (β = 0.33) for the oxidation of **3A** to **3C**$^+$ enables one to obtain the electron-transfer rate constant for this process. Simulations of CV data (Figure 5) over scan rates from 0.4 to 2 V s^{-1} gave a k_s value of 0.009 cm s^{-1}.[31,32] The simulation parameters used for the *cathodic* process (**3B**$^+$/**3C**) on the return sweep are not unique, since an independent measure of $E_{1/2}$ (**3B**$^+$/**3C**) was not obtained. Only ranges of values can be obtained for the cathodic process because various combinations of $E_{1/2}$ and k_s account for its features. It appears, however, that $E_{1/2}$ (**3B**$^+$/**3C**) is between −0.11 V and −0.32 V.[33] Changing the rate constants of the coupled chemical reactions (**3C**$^+$ → **3B**$^+$ and **3C** → **3A**) between 10^3 s^{-1} and 10^8 s^{-1}did not alter the simulations. Because rate constants lower than 10^3 s^{-1} did not agree with experiment, this value can be taken as the lower rate limit of the structural rearrangement steps.

Table 2. Values of k_f (eq B) for the Homogeneous Redox Catalysis of **3** in CH_2Cl_2/0.1 M $[NBu_4][PF_6]$, T = Ambient

mediator (Q)	$E_{1/2}$ of mediator[a]	k_f ($M^{-1}s^{-1}$)	experimental method
$[Pd\{S_2C_2(CN)_2\}_2]^-$	−0.09	6×10^3	steady state, working curves[b]
Ferrocene	0	2×10^5	CV, simulations
Ferrocenylacetonitrile	0.07 V	1×10^7	CV, working curves[c]

[a] Volt vs $[FeCp_2]^{0/+}$. [b] Ref 19a. [c] Ref 19b.

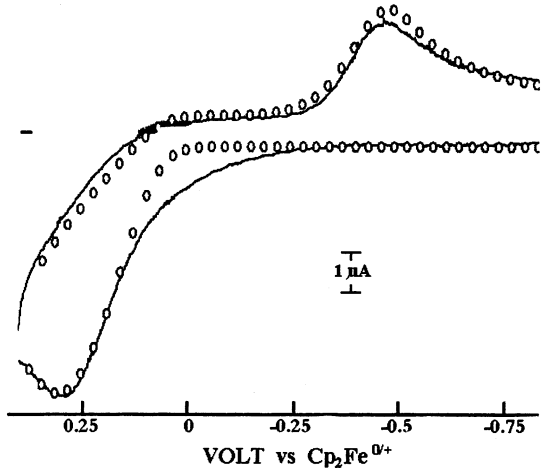

Figure 5. Comparison of representative experimental and simulated data for $[Rh(CO)(PCy_3)Tp^{Me2}]$ (**3**) under conditions similar to those of Figure 2, scan rate 2 V s^{-1}. Simulation parameters: $E_{1/2}$ (**3A**/**3C**$^+$) = 0.20 V, β = 0.33, k_s = 9×10^{-3} cm s^{-1}; $E_{1/2}$ (**3B**$^+$/**3C**) = −0.31 V, α = 0.45, k_s = 4×10^{-3} cm s^{-1}, forward reaction rates of C steps: for E_{ox}C, 10^3 s^{-1}; for E_{red}C, 10^2 s^{-1}. R_u = 4000 Ω, C_d = 0.15 μF.

$[Rh(CO)\{P(OPh)_3\}Tp^{Me2}]$ (1) and $[Rh(CO)(PPh_3)Tp^{Me2}]$ (2): Quasi-Nernstian Systems. Compounds **1** and **2** display almost fully reversible one-electron behavior under conditions of slow CV scan rates at room temperature (Figure 6). At higher scan rates, the peak separations (ΔE_p values) increased over those of a nernstian system, allowing an estimate of the

(31) Best fits required very small changes in simulation parameters (0.01 V in $E_{1/2}$, 0.01 in β, 0.001 in k_s.

(32) The slow anodic rise was not observed when the supporting electrolyte was 0.05 M $[NBu_4][B(C_6F_5)_4]$, but the main features of the CV remained unchanged.

(33) This $E_{1/2}$ range is based on the following points. A cathodic wave exhibiting e.t. irreversibility at a scan rate of 2 V s^{-1} must have a k_s value of no more than about 0.005 cm s^{-1} under these experimental conditions. The measured E_{pc} value of −0.45 V at this scan rate requires an $E_{1/2}$ that is no more negative than −0.32 V, which can be viewed as the thermodynamic lower limit of the **3B**$^+$/**3C** couple. The upper "limit" of −0.11 V was obtained by estimating, without experimental confirmation, a kinetic lower limit of k_s for this reaction as 10^{-4} cm s^{-1}.

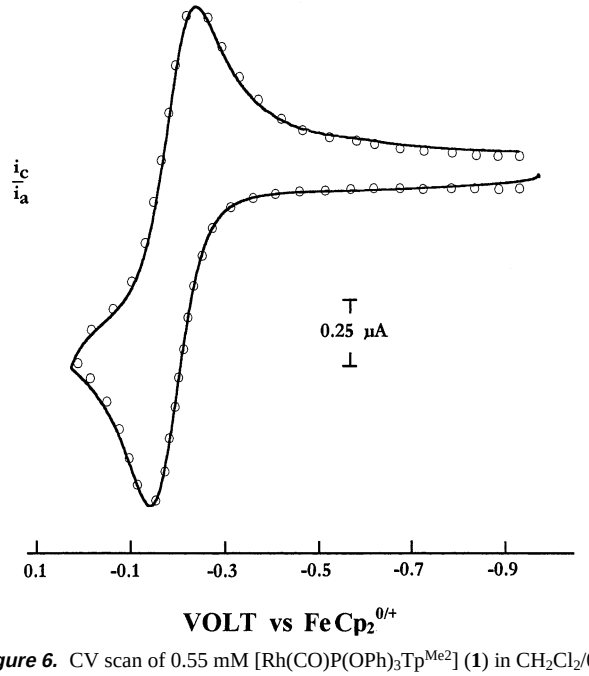

Figure 6. CV scan of 0.55 mM [Rh(CO)P(OPh)$_3$Tp^{Me2}] (**1**) in CH_2Cl_2/0.1 M [NBu_4][PF_6] at glassy carbon electrode, $T = 295$ K, scan rate 0.2 V s^{-1}. Simulated curve shown as circles, $k_s = 0.025$ cm s^{-1}, $\alpha = 0.5$.

heterogeneous electron-transfer rate constant, k_s,[34] of 0.025 cm s^{-1} for **1** and 0.015 cm s^{-1} for **2**. Digital simulations using these k_s values and $E_{1/2}$ values of −0.17 V and −0.25 V for **1** and **2**, respectively, were in close agreement with experiment (Figure 6). Under these experimental conditions, the redox mechanisms of **1**$^{0/+}$ and **2**$^{0/+}$are adequately modeled as single-step E_{QN} (quasi-nernstian) processes, i.e., the diagonal electron-transfer process of Scheme 1.[35]

These results do not, however, rule out a pair of two-step processes for **1** or **2** in which *both* the E and C steps are fast on the CV time scale.[36] Because the overall redox process involves a change from the κ^2-ligation of Tp^{Me2} in the neutral Rh(I) compounds to κ^3-ligation in the Rh(II) cations, we conclude that it is with relative ease that compounds **1** and **2** undergo the electron-transfer induced Rh−N(2) bond formation and cleavage processes.

[Rh(PPh$_3$)$_2$Tp^{Me2}] (4). The voltammetric behavior of the bis-(triphenylphosphine) complex **4** is generally similar to that of **3**, in that the diagnostics are consistent with an overall chemically reversible one-electron $E_{ox}C/E_{red}C$ mechanism in which the charge-transfer steps are rate determining. From the variations of E_p with CV scan rate, the transfer coefficients were measured as $\beta = 0.34$ for **4A**/**4C**$^+$ and $\alpha = 0.45$ for **4B**$^+$/**4C**. A difference of no more than 120 mV is estimated for $E_{1/2}$ values of the oxidation and reduction couples, with k_s ranges of 0.002 to 0.0007 cm s^{-1} for **4A**/**4C**$^+$ and 0.004 to 0.0001 cm s^{-1} for **4B**$^+$/**4C**, using logic similar to that described above for **3**. One of the simulations of this system is shown in Figure 7. The lower limits of the rates of the coupled chemical reactions (**4C**$^+$→ **4B**$^+$ and **4C**→ **4A**) are 10^4 s^{-1}.

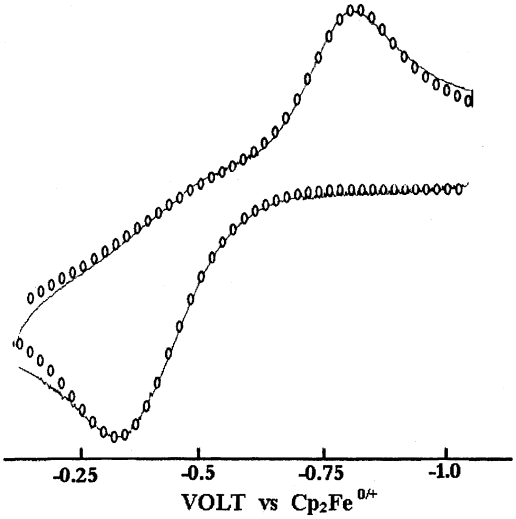

Figure 7. Comparison of representative experimental and simulated data for [Rh(PPh$_3$)$_2$Tp^{Me2}] (**4**) under conditions similar to those of Figure 2, scan rate 1 V s^{-1}. Simulation parameters: $E_{1/2}$ (**4A**/**4C**$^+$) = −0.58 V, $\beta = 0.35$, $k_s = 1 \times 10^{-3}$ cm s^{-1}; $E_{1/2}$ (**4B**$^+$/**4C**) = −0.77 V, $\alpha = 0.45$, $k_s = 1 \times 10^{-3}$ cm s^{-1}, forward reaction rates of C steps: for $E_{ox}C$, 10^4 s^{-1}; for $E_{red}C$, 10^2 s^{-1}. $R_u = 4000$ Ω, $C_d = 0.1$ μF.

Discussion

We first consider what the measured intrinsic charge-transfer rate for the oxidation of **3A** ($k_s = 0.009$ cm s^{-1}) implies about the structural reorganization in the process **3A** -e$^-$ → **3C**$^+$. The activation free energy barrier, ΔG^*, for the electron-transfer process is the sum of the outer-sphere and inner-sphere terms, ΔG^*_{outer} and ΔG^*_{inner}, respectively. The former is dominated by solvation effects, expected to be ca. 5 kcal mol^{-1} under these conditions.[37] The measured value of $\Delta G^* = 8.1$ kcal mol^{-1} therefore implies a ΔG^*_{inner} value of ca. 3 kcal mol^{-1} for **3A** −e$^-$ → **3C**$^+$ and an inner-sphere reorganizational energy (λ_{inner}, eq 6)[38] of ca.12 kcal mol^{-1}. This value, while considerable (λ_{inner} for [$FeCp_2$]$^{0/+}$ is < 1 kcal mol^{-1}),[39] is far too small to describe an electron-transfer involving the making of a strong Rh−N(2) bond

$$\lambda_{inner} \cong 4\Delta G^*_{inner} \qquad (6)$$

A further structural change (and second transition state) is clearly needed to complete the forward reaction, culminating in the $E_{ox}C$ process of eq 7

$$\mathbf{3A} \xrightarrow{E_{ox}} \mathbf{3C}^+ \xrightarrow{C} \mathbf{3B}^+ \qquad (7)$$

By similar reasoning, the complete reverse reaction for the PCy_3 derivative **3** must occur through the $E_{red}C$ mechanism of eq 8

$$\mathbf{3B}^+ \xrightarrow{E_{red}} \mathbf{3C} \xrightarrow{C} \mathbf{3A} \qquad (8)$$

The key to understanding differences in the voltammetric behavior of this group of molecules lies, we believe, in the nature of the structural changes necessary to go from stable reactant to stable product (in this case **3A** to **3B**$^+$) and back. Note that

(34) See ref 17(b). For example, at a scan rate of 2 V s^{-1}, the iR_u-corrected ΔE_p was 90 mV for **1**.
(35) Simulations of data at 273 K were best fit by $k_s = 0.015$ cm s^{-1} and $\beta = 0.35$. The β value was taken from the shape of the anodic wave at 243 K using $E_p - E_{p/2} = 38/\beta$ mV.
(36) Digital simulations with relatively rapid electron-transfer and chemical follow-up reactions gave reasonable fits with experiment.
(37) Weaver, M. J.; Gennett T. *Chem. Phys. Lett.* **1985**, *113*, 213.
(38) $\lambda_{inner} = 4\ \Delta G^*$ when ignoring work terms: see Hale, J. M. In *Reactions of Molecules at Electrodes*; Hush, N. S., Ed.; Wiley-Interscience: New York, 1971; pp 229 ff. Following Hale, we use a preexponential factor of 10^4 in converting k_s to ΔG^*.
(39) Gennett, T.; Weaver, M. J. *J. Electroanal. Chem.* **1985**, *186*, 179.

Table 3. Summary of Electron-Transfer Properties of Hydrotris(pyrazolyl)Boratorhodium Complexes in CH_2Cl_2/0.1 M $[NBu_4][PF_6]$ at Glassy Carbon Electrode

redox process	$E_{1/2}$ (or E_p)[a]	k_s (cm s^{-1})	transfer coeff	$\Delta G^{\ddagger}$[b]
$[Rh(CO)\{P(OPh)_3\}Tp^{Me2}]$, **1** ⇌ **1**$^+$	−0.17	0.025	*c*	7.5[d]
$[Rh(CO)(PPh_3)Tp^{Me2}]$, **2** ⇌ **2**$^+$	−0.25	0.015	$\beta = 0.35$[e]	7.2_5[f]
$[Rh(CO)(PCy_3)Tp^{Me2}]$, **3A** → **3C**$^+$	0.20[g]	0.009	$\beta = 0.33$	8.1[d]
$[Rh(CO)(PCy_3)Tp^{Me2}]$, **3B**$^+$ → **3C**	(E_{pc} ca. −0.45)[h]	*c*	$\alpha = 0.47$	
$[Rh(PPh_3)_2Tp^{Me2}]$, **4A** → **4C**$^+$	(E_{pa} ca. −0.5)[h]	*c*	$\beta = 0.34$	
$[Rh(PPh_3)_2Tp^{Me2}]$, **4B**$^+$ → **4C**	(E_{pc} ca. −0.8)[h]	*c*	$\alpha = 0.45$	

[a] Volt vs $[FeCp_2]^{0/+}$. [b] kcal/mol. A preexponential factor of 10^4 was used. [c] Experimental conditions insufficient to measure this parameter. [d] $T = 295$ K. [e] Transfer coefficient taken from anodic wave shape at 243 K. [f] $T = 273$ K. [g] Measured as 0.21 V by homogeneous redox catalysis, 0.20 V by simulations. [h] Scan rate dependent.

Scheme 3

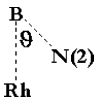

in going from the neutral compound to the stable cation, $[Rh(CO)(PCy_3)Tp^{Me2}]$ must undergo a large change in *both* the Rh−N(2) bond length and the Rh···B−N(1)−N(2) torsion angle (Scheme 3). The latter is 0° for an ideal square pyramid. The very large torsion angle of **3A** (103°) originates from the steric effect which maximizes the distance between the bulky phosphine ligand and the 5-methyl substituent on the ring.[14] It is likely, therefore, that E_{ox} (**3A**/**3C**$^+$) involves torsional rotation of the third pyrazolyl ring allowing a weak Rh−N(2) interaction, after which there is rapid completion of the Rh−N(2) bond in the C step. The low transfer coefficient for **3A**/**3C**$^+$ ($\beta = 0.33$) implies certain properties about the transition state structure for the E_{ox} step. A common interpretation of transfer coefficients below 0.5 is that the transition state lies closer in the reaction coordinate to the product than to the reactant.[40] Application to the present case is consistent with a transition state structure (**3C**$^+$) lying closer to the five-coordinate geometry of **3B**$^+$ than to four-coordinate **3A**. Although the exact structure of **3C**$^+$ cannot be determined by these experiments,[41] a pseudo-square pyramidal model is consistent with the available data and with the known structural tendencies of this series of compounds.

It is noteworthy that the λ_{inner} values for compounds **1** and **2** are also in the 11−12 kcal mol^{-1} range based on the ΔG^* values of Table 3. Because **1** has a less sterically hindering phosphite ligand, its torsion angle (19°) is much lower, even though the metal-nitrogen distance of 2.764 Å is still insufficient to signify more than weak Rh−N(2) bonding (cf. 3.925 Å in **3**, 2.224 Å in **2**$^+$).[22] Relevant to the present discussion is the fact that significant lowering of the Rh···B−N(1)−N(2) torsion angle occurs *without* formation of a Rh−N(2) interaction that is strong enough to signify κ^3-coordination. Within this model, compound **1** might be expected to bypass the two-step E_{ox}C process because it already possesses a pseudo-square pyramidal Rh(I) structure. This is supported by the present experiments, which show that a single-step quasi-nernstian (E_{QN}) process accounts for the voltammetric behavior of **1**/**1**$^+$. It must be emphasized, however, that the data for **1**/**1**$^+$ apply to a narrow range of experimental conditions, and that investigations under more testing time and temperature conditions might shed further light on this process.

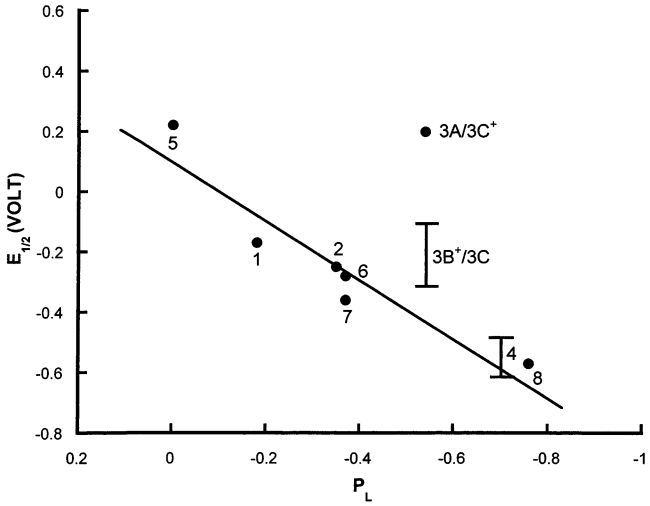

Figure 8. Plot of measured or estimated $E_{1/2}$ values vs. ferrocene for $[RhLL'Tp^{Me2}]$ one-electron oxidations in CH_2Cl_2/0.1 M $[NBu_4][PF_6]$ as a function of ligand electronic parameter P_L,[42b] See text for source of bracketed (estimated) values. Legend: compounds **1**−**4** as defined in this paper; **5** = $[Rh(CO)_2Tp^{Me2}]$; **6** = $[Rh(CO)\{P(tolyl\text{-}m)_3\}Tp^{Me2}]$; **7** = $[Rh(CO)\{P(NMe_2)_3\}Tp^{Me2}]$; **8** = $[Rh(PPh_3)_2Tp]$. The line is the least-squares fit for compounds **1**, **2**, and **5**−**8**.

The torsion angles of **2** (90°) and **4** (75°), as well as their Rh−N(2) distances (3.357 Å and 3.276 Å, respectively), place their structures somewhere between those of compounds **1** and **3**. The CV behavior of the bis(triphenylphosphine) derivative **4** is very similar to that of **3**, showing a pair of two-step processes with β and α values virtually identical to those of **3**. Although compound **2** shows close-to-nernstian behavior, further interpretation of its voltammetry requires more information than is presently available.

The thermodynamics of the e.t. reactions also help inform the discussion. Figure 8 presents the $E_{1/2}$ values under similar conditions for nine members of this series,[42] plotted against the ligand electronic parameter[43] P_L. Two of the values, namely those of **3B**$^+$/**3C** and **4**/**4**$^+$, are entered with error bars based on estimates derived from the discussions above. The other values lie within acceptable agreement with linearity, with one exception, namely **3A**/**3C**$^+$, for which the $E_{1/2}$ is over 600 mV positive of the expected value. It appears that the PCy_3 ligand has the effect of significant *thermodynamic destabilization* of the cationic intermediate **3C**$^+$ that arises from steric rather than

(40) See ref 1, pp 97−98.
(41) The intermediate (**C**-type) structures must differ from the **B**- and **A**-type structures by more than just the Rh−N(2) bond length, since such a restriction would lead to the unlikely model that the intermediates and products are bond-length isomers. The pseudo square-pyramidal structure avoids this, as would other reasonable structures such as that of the trigonal pyramid.
(42) Data taken from ref 14, from Table 1, and from Yeomans, B., unpublished work.
(43) The ligand electronic parameters used in Figure 8 are derived from two sources: Rahman, M. M.; Liu, H.-Y.; Eriks, E.; Prock, A.; Giering, W. P. *Organometallics*, **1989**, *8*, 1 (b) Chatt, J.; Kan, C. T.; Leigh, G. J.; Pickett, C. J.; Stanley, D. R. *J. Chem. Soc., Dalton Trans.* **1980**, 2032. See also Lever, B. *Inorg. Chem.* **1990**, *29*, 1271, and references therein.

Scheme 4

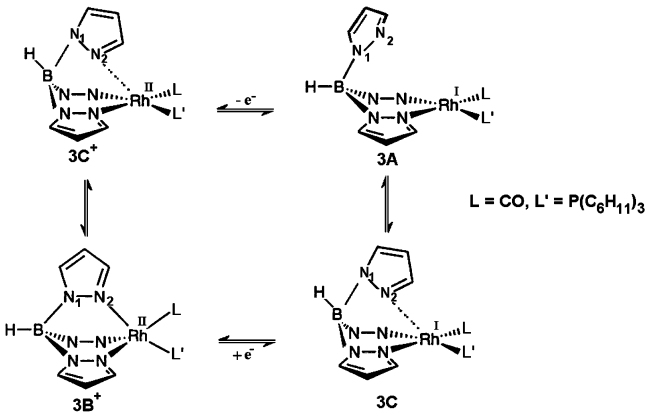

electronic sources. Although $E_{1/2}$ of the cathodic process involving reduction of the 17 e$^-$ cation **3B**$^+$ is still not accurately known, it appears to be much closer to the potential expected for **3**/**3**$^+$ strictly on the basis of electronic effects.

Relevance to the Bond Alteration Model. The traditional square scheme of Scheme 1 is the starting point for understanding the disparate voltammetric behavior of RhTp^{Me2} complexes **1**−**4**, which are rationalized in terms of ligand steric factors that may inhibit structural rearrangements in the charge-transfer steps. Compounds **3** and **4**, which contain bulkier ligands, both undergo a chemically reversible two-step reaction in an overall $E_{ox}C/E_{red}C$ process drawn specifically for **3** in Scheme 4. In the structural reorganization for $E_{ox,}$ the previously uncoordinated pyrazolyl ring in **3A** rotates about B−N(1) and bends toward the metal, thereby decreasing the Rh···B−N(1)−N(2) torsion angle and increasing the Rh- - -N(2) interaction in **3C**$^+$. This reorganization effectively facilitates the subsequent bond-making step (chemical step, C) in which the 15-electron Rh(II) cation coordinates N(2) by accepting a lone pair into its d_z^2 orbital, completing the apical Rh−N(2) interaction in the 17-electron monocation **3B**$^+$. The reverse process occurs in the reduction of **3B**$^+$ back to 16-electron **3A**.[44] Viewed in the oxidative direction, electron transfer is an associative (bond-making) process, whereas in the reductive direction it is a dissociative (bond-breaking) process. By way of contrast, concerted bond alteration processes cannot be ruled out for compounds **1** and **2**. Their quasi-nernstian behavior can be accounted for by either a single-step process or a square scheme in which both the charge-transfer and chemical steps are fast on the CV time scale.

The two-step bond cleavage reactions seen for the reductions of **3B**$^+$ and **4B**$^+$ may be seen as analogous to the Savéant model of dissociative e.t. for organic halides. In that case, one-electron reduction of RX may proceed by a two-step process if "the unpaired electron located in one portion of the molecule dissociatively reduces a bond belonging to the same molecule".[5] In the present case, the one-electron reduction of **3B**$^+$ to **3A** places *two* electrons in a Rh−N σ^* bond,[14] thereby facilitating transfer of the *lone pair* from the 18-electron Rh(I) back to the nitrogen, resulting in Rh−N(2) bond cleavage. The cathodic processes therefore allow inquiries similar to those being addressed in organic models of dissociative electron-transfer reactions.[2e,5,6,9]

(44) We invoke the general principle of microscopic reversibility.

There is far less precedent for anodic associative reactions. Concerted e.t. and bond *formation* has been invoked to account for the *inter*molecular oxidation of some simple anions such as I$^-$ and [SCN]$^-$.[45] Among *intra*molecular processes, we draw attention to "base-off, base-on" conversions in the redox chemistry of vitamin B_{12} derivatives.[46] One must also consider the metal π-hapticity changes noted in the Introduction and anodic reactions that are accompanied by metal−metal bond formation. A number of the latter have been found for fulvalenediyl-systems or other complexes in which two metals are bridged by a π-ligand.[47] In many cases, however, these systems are subject to "inverted" two-electron couples[48] which add significantly to the complexity of the mechanistic questions.

Among other relevant studies[49] is the work of Harmon, Taube, and co-workers on the redox-induced linkage isomerizations of organometallic osmium complexes.[50] When the Os(II) compound $[Os(NH_3)_5L]^{2+}$ is oxidized to the corresponding Os(III) trication, certain ligands (L) undergo a change in hapticity, for example from an η^2-bonded arene to a κ^1-bonded oxygen in L = methylbenzoate.[51] Whereas detailed mechanistic work has not been reported on the redox chemistry of these systems, a square scheme has been invoked to rationalize the overall behavior. The osmium systems exhibit, on occasion, grossly irreversible electrochemical behavior,[50(b),51] although the probable transition state structure is not obvious.

It is clear that structural, bonding, and medium effects may all influence the mechanism of dissociative and associative e.t.reactions. Information on the role of *steric factors* in such reactions is sparse.[52,53] Certainly, systems in which the molecular factors may be controlled give an advantageous starting point. There exists an abundant literature demonstrating how substituents on the pyrazolyl rings influence the metal−ligand bonding and the structural preferences of tris(pyrazolyl)borate complexes.[16] This class of compounds appears, therefore, to be well suited to support systematic probes of how combined steric and electronic effects influence fundamental aspects of e.t. reactions.

Summary

The chemically reversible one-electron oxidations of [RhLL′Tp^{Me2}] complexes **1**−**4** demonstrate qualitatively different CV behavior. For compounds **3** and **4**, the electron-transfer steps of both the original oxidation and the subsequent rereduction are rate limiting, giving rise to totally irreversible heterogeneous charge-transfer processes. Their behavior is

(45) Hung, M.-L.; Stanbury, D. M. *Inorg. Chem.* **1994**, *33*, 4062, and references therein.
(46) Lexa, D.; Savéant, J.-M. *Acc. Chem. Res.* **1983**, *16*, 235.
(47) (a) Connelly, N. G.; Lucy, A. R.; Payne, J. D.; Galas, A. M. R.; Geiger, W. E. *J. Chem. Soc., Dalton Trans.* **1983**, 1879. (b) Freeman, M. J.; Orpen, A. G.; Connelly, N. G.; Manners, I.; Raven, S. J. *J. Chem. Soc., Dalton Trans.* **1985**, 2283. (c) Chin, T. T.; Geiger, W. E.; Rheingold, A. L *J. Am. Chem. Soc.* **1996**, *118*, 5002. (d) Moulton, R.; Weidman, T. W.; Vollhardt, K. P. C.; Bard, A. J. *Inorg. Chem.* **1986**, *25*, 1846. (e) Brown, D.; Delville-Desbois, M. H.; Vollhardt, K. P. C.; Astruc, D. *New J. Chem.* **1992**, *16*, 899. (f) Geiger, W. E.; Salzer, A.; Edwin, J.; von Philipsborn, W.; Piantini, A. L. R. *J. Am. Chem. Soc.* **1990**, *112*, 7113.
(48) Entries a−d of ref 47 refer to net two-electron processes.
(49) (a) Kuchynka, D. J.; Kochi, J. K. *Inorg. Chem.* **1988**, *27*, 2574. (b) Delville-Desbois, M.-H.; Mross, S.; Astruc, D.; Linares, J.; Varret, F.; Rabaâ; Le Beuze, A.; Saillard, J.-Y.; Culp R. D.; Atwood, D. A.; Cowley, A. H. *J. Am. Chem. Soc.* **1996**, *118*, 4133.
(50) (a) Harmon, W. D.; Taube, H. *J. Am. Chem. Soc.* **1987**, *109*, 1883. (b) Harmon, W. D.; Sekine, M.; Taube, H. *J. Am. Chem. Soc.* **1988**, *110*, 2439.
(51) Nunes, F. S.; Taube, H. *Inorg. Chem.* **1994**, *33*, 3111.
(52) Geue, R. J.; Hanna, J. V.; Hohn, A.; Qin, C. J.; Ralph, S. F.; Sargeson, A.; Willis, C. A. In *Adv Chem Ser*; Isied, S., Ed.; **1997**, *253*, 137.
(53) Anne, A.; Fraoua, S.; Grass, V.; Moiroux, J.; Savèant, J.-M. *J. Am. Chem. Soc.* **1998**, *120*, 2951.

modeled by an $E_{ox}C/E_{red}C$ square scheme with each redox reaction being a two-step (sequential) process. The overall processes comprise a reversible sequence of *intramolecular associative and dissociative* e.t. reactions involving formation and cleavage, respectively, of the Rh−N(2) apical bond. In contrast, compounds **1** and **2** display quasi-nernstian behavior for which either a single-step (concerted) process or a sequential $E_{ox}C/E_{red}C$ process composed of relatively fast reactions are possible. Structural differences provide a rationale for the results. The bulky L and L′ ligands in **3** and **4** impose steric constraints both on the electron-transfer process and on the subsequent formation of a Rh−N(2) bond necessary to give the square pyramidal cationic Rh(II) oxidation product. In the case of **1**, the Rh d_z^2 orbital is already pointed toward N(2), minimizing the rearrangement energy necessary to form the Rh-apical N(2) bond.

Acknowledgment. This work was supported by the U.S. National Science Foundation and by the EPSRC. W.E.G. is grateful to the School of Chemistry at the University of Bristol for hospitality during a sabbatical leave and to the Leverhulme Trust and the Benjamin Meaker Fund for support during that period. We also thank reviewers for comments and suggestions.

JA0302073